Jurnal Kejuruteraan 37(1) 2025: 25-36
https://doi.org/10.17576/jkukm-2025-37(1)-03

Empirical Evaluation and Parametric Optimization of Stepped Versus Traditional Solar Stills using Taguchi's Methodology

Krunalkumar B Patel[a,b*] & Tushar M Patel[a,c]

[a]*Mechanical Engineering Department Programme,*

[b]*Kadi Sarva Vishwa Vidyalaya, Gandhinagar, Gujarat, India.*

[c]*LDRP-ITR, Gandhinagar, Gujarat, India.*

[*]*Corresponding author: krunalpatel31185@gmail.com*

Received 15 May 2024, Received in revised form 4 July 2024
Accepted 4 August 2024, Available online 30 January 2025

ABSTRACT

The escalating scarcity of potable water in remote and arid regions necessitates increased reliance on sustainable solutions, notably solar stills. The imperative need to achieve high productivity and peak hour effi ciency in these devices is critical to eff ectively addressing water shortages. This study explored modifi ed solar still designs aimed at improving the productivity and peak-hour effi ciency of the water desalination process. The experimental investigations involved various parameters, including water depth (10, 20, and 30 mm), mass fl ow rate (10, 15, and 20 kg/h), and glass thickness (4, 5, and 6 mm) for both traditional and stepped solar stills. The experimental layout followed an L18 orthogonal array. It was structured with $2^1 \times 3^3 = 18$ combinations, ensuring comprehensive coverage of the factors and levels involved, and the outputs were systematically examined using the Taguchi approach to identify the optimal parameter values. Stepped solar stills have emerged as superior, demonstrating higher peak-hour effi ciency and productivity than traditional solar stills. The most infl uential parameters, ranked by eff ectiveness, were the type of solar still, water depth, glass thickness, and mass fl ow rate. The optimal conditions for achieving maximum productivity (3881 ml) and peak hour effi ciency (22.03%) were identifi ed, including a stepped solar still, 10 mm water depth, 15 kg/h mass fl ow rate, and 4 mm glass thickness. The experimentally measured values were closely aligned with the predicted values, verifying the accuracy of the Taguchi model with minimal error (0.81% in productivity and 0.49% in peak hour efficiency).

Keywords: Desalination; water distillation; solar energy; traditional solar still; stepped solar still; saline water

INTRODUCTION

Water, the essence of life, remains a fundamental resource crucial for the sustenance of all living organisms (Malik et al. 1982). Purified water is essential for sustaining respiratory processes among organisms in natural ecosystems. Despite water covering over 97% of Earth's surface, a considerable portion is saline, with only 3% classified as freshwater, of which a mere 1% is easily accessible to humans (Tiwari, Singh and Tripathi 2003; Modi and Modi 2019). The continuous decline in potable water availability is attributed to an ever-growing global population and pollution from natural sources. This poses a significant challenge for humanity. The exponential increase in the global population and pollution from existing water sources have significantly contributed to the critical shortage of clean water (Jani and Modi 2017; Jani and Modi 2018). A substantial proportion of the world's inhabitants lack access to safe and clean drinking water, leading to waterborne diseases that affect more than 60 lakh children annually (Dwivedi and Tiwari 2009). Impure water often carries diseases, bacteria, parasites, unidentified substances, physical pollutants, and synthetic contaminants, posing serious threats to human hygiene (Dwivedi and Tiwari 2009; Manikandan et al. 2013; Rahbar, Esfahani and Asadi 2016). Consequently, there is a pressing need to purify water obtained from various wetlands and non-wetland waters such as streams, lakes, oceans, and rainfall

(Nayi and Modi 2019; Modi and Nayi 2020; Modi, Nayi and Sharma 2020; Nayi and Modi 2021). Solar-powered purification has become an effective method for purifying water (Jani and Modi 2019). As a beacon of hope amid escalating water scarcity and pollution, solar desalination stands out for its simplicity and efficiency, harnessing solar energy to convert saltwater into potable freshwater. Designed specifically for this purpose, solar stills offer versatile applications across industrial and domestic settings, showcasing the potential of solar energy as a sustainable and environmentally friendly solution for desalting seawater.

In practical scenarios, the focus is on the ingenuity and technological advancements of any system with the goal of enhancing reliability, affordability, and efficiency. This approach has prompted engineers and designers to create a variety of innovative and efficient solar-still configurations that surpass traditional solar-stills in terms of both output and cost-effectiveness (Yadav and Sudhakar 2015; Sathyamurthy et al. 2015; Kabeel et al. 2019). Many attempts have been made to improve the output of solar stills by incorporating supplementary systems. These initiatives aim to improve performance of solar stills through synergistic combinations with other solar technologies and complementary systems (Kumar et al. 2015; Rufuss et al. 2016). In a noteworthy study of an innovative solar still, Hansen and Murugavel (2017) sought to improve the output of an inclined solar still integrated with a heated water reservoir and a basic solar still. Cascade solar stills have garnered significant attention from researchers including Tabrizi et al. (2010), Elshamy and El-said (2018) and Patel et al. (2021). The condensation and evaporation rates significantly influence the production of solar stills. Various arrangements, like including fins and wicks into the basin liner or constructing a concave basin surface, have been proposed to enhance the evaporation area. Semi-circular corrugated wicks have demonstrated superior performance, offering a larger rate of evaporation than flat corrugated wicks, owing to their larger evaporation surface. For example, a solar still with semicircular corrugations yielded 4.3 kg/m^2, while a flat-plate corrugated absorber yielded 3.4 kg/m^2. The semi-circular corrugated configuration exhibited better energy efficiency and lower water production costs. Grewal and Kumar (2022a) explored an energy recovery system comprising three-stepped solar stills with concentrated sugarcane juice using an experimental setup. Optimal performance was observed at 0.05 kg/min, achieving a maximum distillate output of 3777.1 g. In a subsequent study, Grewal and Kumar (2022b) used phase-change energy storage material in different masses within stepped solar stills. The highest efficiency was achieved with SERS-ESM60, producing 2175.6 g and 25.8^o brix content. Grewal and Kumar (2022c) investigated concentrated stepped solar stills loaded with various energy-storage materials (ESM) in 15, 30, and 60 Cu tubes. This study revealed that ESM60 exhibited the highest efficiency, yielding 2486.1 a of distillate output. Thakkar, Mevada and Panchal (2024) enhanced solar desalination by integrating flashing of solar-heated water, achieving a 38% increase in distillate yield by optimizing water flow rates and system design.

Various optimization and statistical methods are employed to anticipate the optimal control parameters and enhance the output with a minimal number of experiments. To ensure the adequacy of the proposed model, the legitimacy of the predicted responses is confirmed through validation tests. Several studies have employed optimization techniques to enhance various processes. Patel and Bhatt (2015) utilized the hybrid FEM and Taguchi methods to reduce the weight of automobile structural component. Ibrahim and Hamza (2017) optimized lipid extraction from municipal waste for the production of biodiesel using the Design of Experiment (DoE) method. Through factorial screening and the Response Surface Method (RSM), they achieved a maximum lipid extraction of 29.4%, highlighting the potential of scum sludge for biodiesel compared to other sources. Berisha, Zeqiri, and Meha (2018) shed light on the optimal tilt angles for solar radiation absorption in Pristina, providing crucial insights into maximizing solar energy utilization. Following this, Ghasempour et al. (2019) explored MCDM methods for site and technology selection in solar plants, emphasizing the importance of informed decision-making amidst environmental concerns and fossil fuel scarcity. Fatriasari et al. (2020) optimized Amphipilic lignin derivatives (A-LD) from Acacia mangium black liquor versus commercial lignin (LS) using the Taguchi method. A-LD, especially A-LD L2S, improved sugar yield during the enzymatic hydrolysis of sweet sorghum bagasse pulp under milder conditions. Ahmed et al. (2020) further contributed by optimizing PV/T solar water collectors using fuzzy logic control, exemplifying real-time feedback mechanisms for efficiency enhancement. Le et al. (2021) reviewed the impact of different basin types on solar still output, emphasizing factors influencing distillation efficiency and recommending strategies for increased productivity. Mugagga, Omosab and Thoruwa (2023) enhanced a water scrubbing system for biogas, attaining over 87% removal of hydrogen sulfide and averaging 77.67% bio-methane content. They utilized the Taguchi method and response surface methodology (RSM) to optimize the liquid flow rate. Du et al. (2023) applied Taguchi's approach for optimizing the process variables of laser cladding for a 15-5PH alloy powder. Karn et al. (2023) focused on optimizing the scratch hardness and micro-hardness achieved using a stabilizer-free electroless nickel-boron bath to remove lead nitrate and heavy metals that pose potential toxicity risks. They utilized the Taguchi method for optimization. Yallese et al. (2023) employed PCA-MARCOS and MARCOS-Taguchi hybrid techniques to optimize the turning parameters of nickel-based super alloy. Abebe and Bogale (2023) optimized the TIG welding process variables for austenitic stainless steel sheet metal using the Taguchi method. The application of the Taguchi method for parametric optimization substantially reduces the number of experimental sets using Design of Experiments (DOE) techniques. In the pursuit of optimizing performance, researchers have delved into various aspects. This literature review encapsulates diverse approaches toward optimization, offering valuable insights for sustainable utilization. Patel, Acharya and Acharya (2024a) employed Taguchi's L9 orthogonal array to optimize Fused Deposition Modeling (FDM) parameters (layer height, infill density, printing speed) for PLA specimens, focusing on improving tensile strength and hardness. Their findings were validated using Taguchi Grey Relation Analysis (TGRA). In a subsequent study by Patel, Acharya and Acharya (2024b), Taguchi Grey Relational Analysis (GRA) was utilized to optimize parameters (infill density, orientation angle, layer height) for PLA components in FDM, leading to overall enhancements in mechanical performance.

In the quest for enhancing the performance and sustainability of solar stills, researchers have explored various parametric optimization strategies. Gnanaraj and Ramachandran (2017) pioneered the optimization of a traditional solar still linked to a solar pond using the Taguchi method, achieving remarkable distillate outputs surpassing conventional stills. Building upon this, Kumar and Kumar (2024) investigated a modified passive solar still (M-SS) in Bareilly, India, integrating nano-enhanced heat storage and fins, showcasing significant advancements in heat yield and environmental impact. Concurrently, Kumaravel, Nagaraj and Barmavatu (2024) delved into improving solar still efficiency by integrating solar ponds and optimizing key parameters, resulting in substantial efficiency gains. This literature review encapsulates innovative approaches towards solar still parametric optimization, highlighting advancements that hold promise for sustainable desalination processes.

The reviewed studies collectively underscore the multifaceted nature of solar still optimization, spanning from tilt angles to basin designs and decision-making frameworks. As the world gravitates towards sustainable energy solutions, the findings presented here offer actionable insights for enhancing solar energy utilization. From Pristina's optimal tilt angles to the intricacies of fuzzy logic control and basin material selection, each study contributes to a comprehensive understanding of how to maximize solar still efficiency. As research in this field progresses, the synthesis of these insights will undoubtedly pave the way for more efficient and sustainable solar energy systems, ultimately driving positive impacts on global energy sustainability.

Despite the wealth of research on solar still optimization, there exists a notable gap concerning the empirical evaluation and optimization of various solar still design parameters like water depth, mass flow rate, and glass thickness using Taguchi's methodology. While previous studies have investigated different configurations and optimization techniques, there remains a need for empirical validation and comparative analysis between stepped and traditional designs. This study seeks to address this gap by providing empirical evidence and optimization insights through Taguchi's methodology, thereby enhancing our understanding of traditional and stepped solar stills' performance and their potential as viable alternatives in solar desalination systems.

EXPERIMENTAL METHODOLOGY

Two solar stills were fabricated for comparative analysis: a traditional solar still and a stepped solar still. Both were directly exposed to sunlight and shared identical variables, such as water depth, mass flow rate, and glass thickness. The solar still was designed as an airtight basin made of mild-steel iron, with the inner surface and absorber plate coated in black to maximize solar radiation absorption. The basin, which was constructed to be airtight, featured an inlet for water and an outlet for water recirculation. A slope was integrated into the basin to maximize solar radiation reception and facilitate the downward flow of water droplets. The setup was oriented southward to receive optimal solar energy throughout the day. Glass was chosen for its high transitivity and low thermal conductivity to transfer maximum radiation into the basin. The basin was sealed airtight using adhesive material or a sealing gasket. External insulation was applied to the outer wall of the basin to minimize heat loss. A water recirculation system was implemented using a pump and buffer tank.

During daylight hours, solar rays penetrate the glass cover, transferring energy to the absorber plate of the basin and increasing the temperature. The water in the basin is heated by convective heat from the absorber plate. As the temperature difference between the water and glass cover increased, water evaporated. In turn, water vapor releases heat at the glass cover, known as the condensing (glass) cover, causing the vapor to condense into droplets on the inner surface of the glass cover. The condensate flows and collects in the channel because of its inclination from the higher side to the lower side. The collected water was then directed through a pure water outlet port and piped into a measuring jar.

The stepped basin solar still was specifically engineered to include a heat storage space within its steps, thereby enhancing productivity over an extended period. Mild steel was used as the construction material, which was consistent with traditional stills. A slope was incorporated into the top of the basin, and a glass cover was fixed atop the basin to facilitate the transfer of radiation. The inner surface was layered with a black coating to maximize the absorption of solar radiation. The temperature sensors were strategically positioned according to the schematic. A water storage tank is situated between the basin and the pump to maintain a constant water level or facilitate the makeup of water inside the basin. The pump draws water from the storage tank and supplies it to the inlet of the basin. The entire setup was directly exposed to sunlight, and data on temperature, distilled water outlet, and solar radiation were recorded throughout the day.

Daily output, solar radiation, and temperature were measured on an hourly and daily basis during daylight. The experimental setup concept is displayed in Figure 1. Various measuring instruments, such as solar power meters, anemometers, temperature sensors at different locations, pH meters, and total dissolve solids (TDS) meters, were used to collect the observational data.

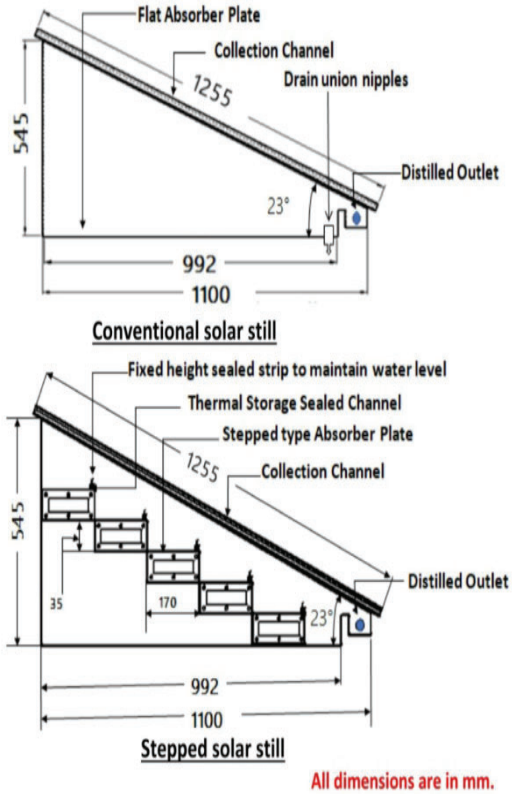

FIGURE 1. Schematic diagram of traditional and stepped solar still

SETTING OF PARAMETERS

WATER DEPTH

In a stepped solar still, installing fixed-height (10 mm, 20 mm, and 30 mm) sealed strips at each step maintains precise water depths. These strips must be carefully measured and positioned to correspond with the desired depths at each step. Verify that the strips are securely sealed to prevent water leakage.

In a conventional solar still, install drain union nipples at designated points within the solar still to facilitate water level adjustment. These nipples should be strategically positioned to correspond with the desired water depths of 10 mm, 20 mm, and 30 mm. Use the drain union nipples to adjust the water level within the solar still to the desired depths of 10 mm, 20 mm, and 30 mm, respectively.

Mass flow rate:

To maintain precise water flow control rates of 10 kg/h, 15 kg/h, and 20 kg/h in a solar still, a meticulous setup is essential. A control valve is strategically positioned at the inlet of the solar still to regulate the flow of water effectively. Upstream from the control valve, a calibrated rotameter is installed to provide continuous monitoring and precise measurement of the flow rates. This setup is complemented by a reliable water source reservoir, guaranteeing a consistent and uninterrupted water supply throughout the experiment.

GLASS THICKNESS

Both solar stills have glass covers of varying thicknesses (4 mm, 5 mm, and 6 mm) in the absorber area according to the requirements of the experiments. Each glass cover should be carefully selected and positioned to correspond with the desired thickness for experimentation. Rubber seals are used around the edges of each glass cover to create an airtight seal in the absorber area. The seals are properly positioned and securely fastened to prevent any air leakage. It is crucial to maintain consistent experimental conditions and prevent any air exchange within the absorber area.

STANDARDIZED CONDITIONS FOR THE EXPERIMENT

To ensure a fair comparison between stepped and conventional solar stills, maintaining standardized conditions throughout the experiment is crucial.

Firstly, both types of solar stills must receive identical sunlight exposure by placing them in the same location and orienting them in the same direction to maximize solar radiation absorption. Secondly, consistency in the water source used for both stills is essential to ensure uniformity in the experiment's conditions, whether it's saline or contaminated water. Applying the same set of parameters to both solar stills establishes a level playing field for comparison. Monitoring and maintaining consistent ambient conditions such as temperature, humidity, and wind speed minimizes external variables that could impact results. Conducting the experiment for the same duration for both solar stills ensures fairness in assessing their performance over time. Employing identical methods for data collection and keeping control variables constant, except for the design of the solar stills, helps isolate the effects of design differences. Ensuring both types of solar stills have the same absorber area, glass inclination, and basin area maintains consistency in receiving identical incident solar radiation and water evaporation rates.

Adhering to these standardized conditions enables researchers to effectively compare the outcomes of stepped and conventional solar stills, ensuring the validity and reliability of the experimental results.

The experiments were conducted in Gandhinagar (23.15° N, 72.66° E), Gujarat, India, from 10 a.m. to 5 p.m. and from April 10, 2023, to April 22, 2023. Initial measurements indicated total dissolved solids (TDS) and pH values of 2130 ppm and 7.8 for saline water and 75–80 ppm and 5.20–5.30 for distilled water.

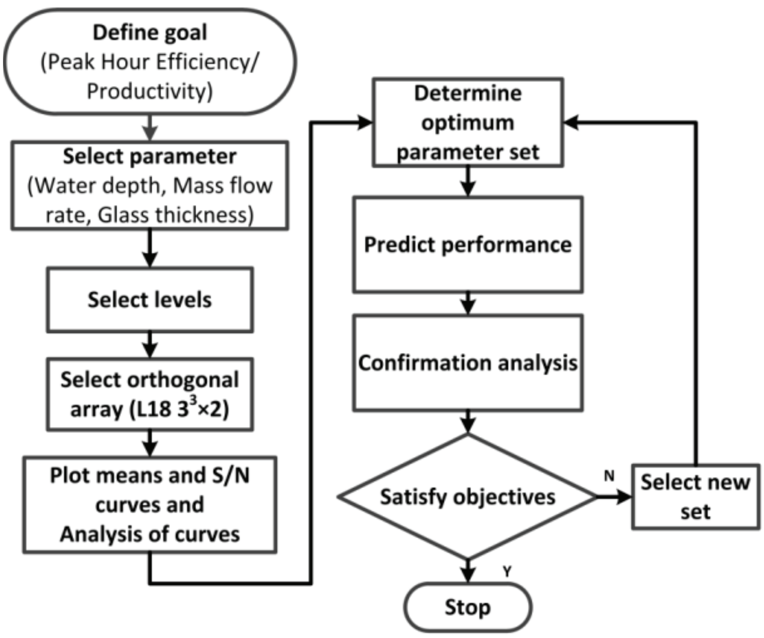

FIGURE 2. Flow chart of experiment

Figure 2 shows the development of an optimization model tailored for the solar still parameters. This model was designed to optimize the critical factors that affect the solar still process, specifically the water depth (mm), mass flow rate (kg/h), and glass thickness (mm). The objective functions for the output parameters are outlined as productivity (ml) and peak hour efficiency (%). A solar still was used to optimize the input parameters. The outcomes of the optimization were subsequently scrutinized through verification experiments and performance tests. Table 1 lists these parameters and their respective levels.

TABLE 1. Parameters and their levels

Parameters	Notations	Unit	Level		
Types of solar still	SS		Traditional (1)	Stepped (2)	
Water depth	WD	mm	10	20	30
Mass flow rate	MFR	kg/h	10	15	20
Glass thickness	GT	mm	0.4	0.5	0.6

MATHEMATICAL MODEL

The productivity is measured at the end of the day using a volumetric measuring beaker. The peak hour efficiency for each experimental set, displayed in Table 2, was calculated using equations suggested by Abdullah (2013). The mathematical modeling steps for the solar still are as follows:

The evaporation heat flux is calculated using the formula (1).

$$q_{ew} = h_{ew}(T_w - T_c) \quad W/m^2 \tag{1}$$

Where, h_{ew} is the coefficient of heat transfer calculated by formula (2),

$$h_{ew} = (16.237 * 10^{-3})\, h_{cw} \frac{(p_w - p_c)}{(T_w - T_c)} \quad W/m^2 K \tag{2}$$

Where, p_w and p_c are the water vapor pressure and the top cover vapor pressure, respectively, calculated by formula (3) and (4), respectively.

$$p_w = e^{(25.317 - 5144/(T_w + 273)} \quad Pa \tag{3}$$

$$p_c = e^{(25.317 - 5144/(T_c + 273))} \quad Pa \tag{4}$$

The water mass produced is calculated using the formula (5).

$$m_{ew} = h_{ew}(T_w - T_c) * \frac{3600}{h_{fg}} \quad kg/m^2.hr \tag{5}$$

The immediate efficiency of the still is calculated using (6).

Where, P_b denotes the power of the blower.

$$\eta = \frac{M \times h_{fg}}{(A \times I \times \Delta t) + P_b} \times 100\ \% \tag{6}$$

The peak hour efficiency (η_{max}) is achieved between 1:00 pm and 2:00 pm when solar radiation is at its maximum.

After finishing the experiment and inputting the data, Minitab gives various graphical and analytical tools to help understand the findings. Taguchi designed experiments using specially designed tables called "orthogonal arrays." The use of these tables simplifies and standardizes the experimental design.

The experimental design employed the mixed Taguchi method to systematically plan trials for each type of solar still. Nine sets of experiments were conducted for every type of solar still, systematically varying key system characteristics: water depth (10, 20, and 30 mm), mass flow rate (10, 15, and 20 kg/h), and glass thickness (4, 5, and 6 mm). The outcomes of these trials, detailing the performance metrics, are presented in Table 2. The experimental layout followed an L18 orthogonal array, structured with $2^1 \times 3^3 = 18$ combinations, ensuring comprehensive coverage of the factors and levels involved.

RESULTS AND DISCUSSION

TAGUCHI MODEL WITH MINITAB16

From Table 2, it can be observed that a minimum productivity value of 1865 ml was obtained in the traditional solar still with a water depth of 30 mm, a mass flow rate of 20 kg/h, and a glass thickness of 5 mm. In contrast, a maximum productivity of 3714 ml was achieved in a stepped solar still applying a water depth of 10 mm, a mass flow rate of 15 kg/h, and a glass thickness of 5 mm.

TABLE 2. Experimental result table

Run	Type of solar still	WD (mm)	MFR (kg/h)	GT (mm)	Productivity (ml)	Ƞmax (%)
1	1	10	10	4	2550	15.8
2	1	10	15	5	2685	15.1
3	1	10	20	6	2340	14.6
4	1	20	10	5	2205	14.3
5	1	20	15	6	2315	14.3
6	1	20	20	4	2520	14.8
7	1	30	10	6	2160	12.8
8	1	30	15	4	2650	15.1
9	1	30	20	5	1865	11.5
10	2	10	10	4	3515	20.9
11	2	10	15	5	3714	21.3
12	2	10	20	6	3315	20.4
13	2	20	10	5	2970	18.8
14	2	20	15	6	3060	18.5
15	2	20	20	4	3365	19.9
16	2	30	10	6	2850	16.7
17	2	30	15	4	3570	19.6
18	2	30	20	5	2765	16.6

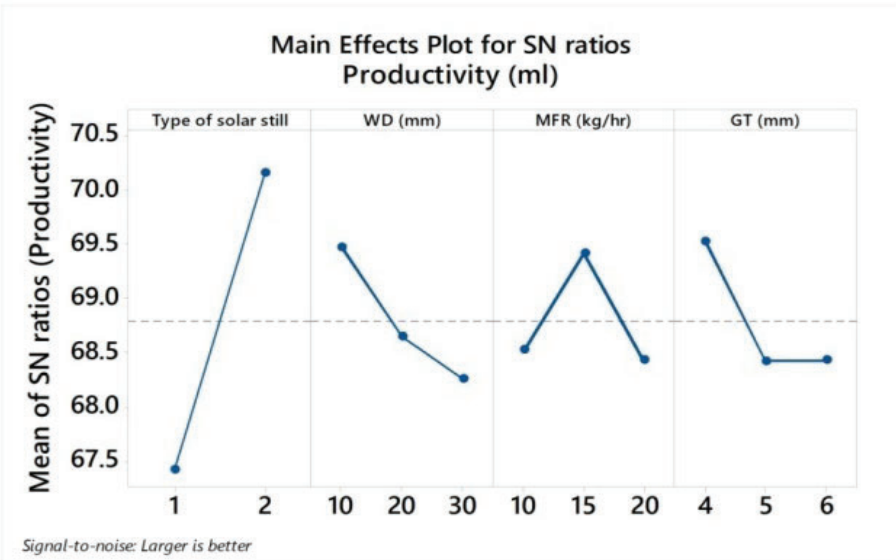

FIGURE 3. Mean of SN ratios for productivity

The mean of the signal-to-noise (SN) ratio for productivity is presented in Figure 3, demonstrating the impact of various factors, including the type of solar still (SS), water depth, mass flow rate, and glass thickness, on productivity. The response table for the SN ratios (larger is better) is presented in Table 3.

TABLE 3. Response table of s/n ratios for productivity

Level	TYPE OF SS	WD (mm)	MFR (kg/h)	GT (mm)
1	67.43	69.47	68.53	69.52
2	70.16	68.65	69.42	68.42
3		68.26	68.43	68.43
Delta	2.73	1.21	0.98	1.10
Rank	1	2	4	3

According to the findings from Response Table 3, the type of solar still had the maximum effect on productivity, whereas the mass flow rate had the minimum effect on productivity. The order of effectiveness of the parameters was as follows: type of solar still (SS) > water depth > glass thickness > mass flow rate.

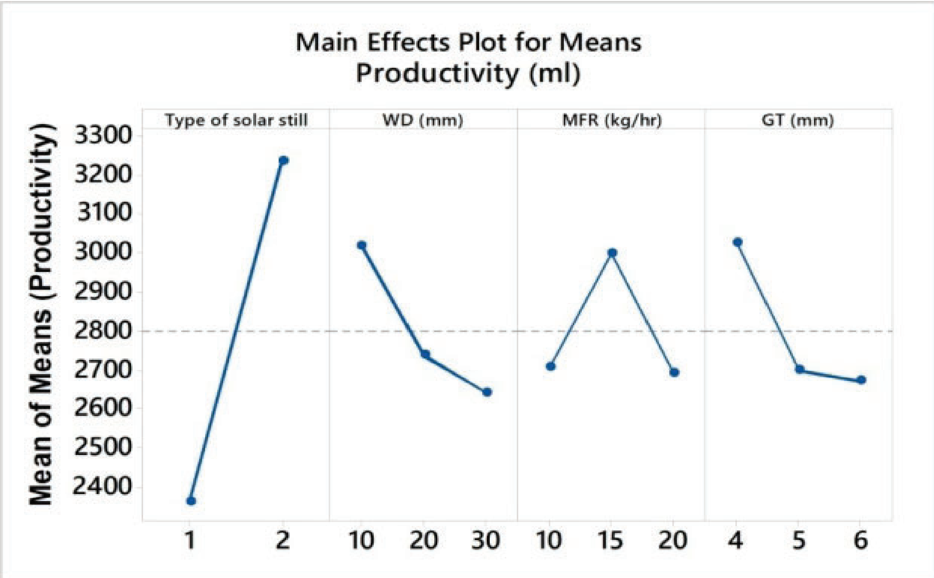

FIGURE 4. Mean of means plot for productivity

Figure 4 displays the main effects plot for means of productivity. It presents the influence of solar still type (SS), water depth, mass flow rate, and glass thickness on productivity on a consistent scale. The response tables for the means are presented in Table 4.

TABLE 4. Response table of means for productivity

Level	TYPE OF SS	WD (mm)	MFR (kg/h)	GT (mm)
1	2366	3020	2708	3028
2	3236	2739	2999	2701
3		2643	2695	2673
Delta	870	377	304	355
Rank	1	2	4	3

Based on the findings from Response Table 4, the solar still type had the maximum effect on productivity, whereas the mass flow rate had the minimum effect on productivity. The order of effectiveness of the parameters was as follows: type of solar still (SS) > water depth > glass thickness > mass flow rate.

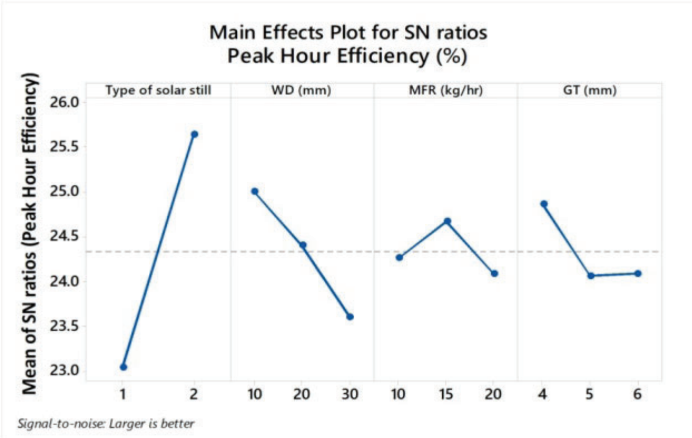

FIGURE 5. Mean of SN ratios for peak hour efficiency

The mean of the SN ratio for peak hour efficiency is presented in Figure 5, which illustrates the impact of various factors, including the type of solar still (SS), water depth, mass flow rate, and glass thickness, on peak hour efficiency. The response table for the SN ratios (larger is better) is presented in Table 5.

TABLE 5. Response table of s/n ratio for peak hour efficiency

Level	TYPE OF SS	WD (mm)	MFR (kg/h)	GT (mm)
1	23.04	25.00	24.26	24.86
2	25.63	24.40	24.67	24.06
3		23.61	24.08	24.09
Delta	2.59	1.39	0.59	0.80
Rank	1	2	4	3

According to the findings from Response Table 5, the mass flow rate had the minimum effect on peak hour efficiency, whereas the type of solar still had the maximum effect on peak hour efficiency. The order of effectiveness of the parameters was as follows: type of solar still (SS) > water depth > glass thickness > mass flow rate.

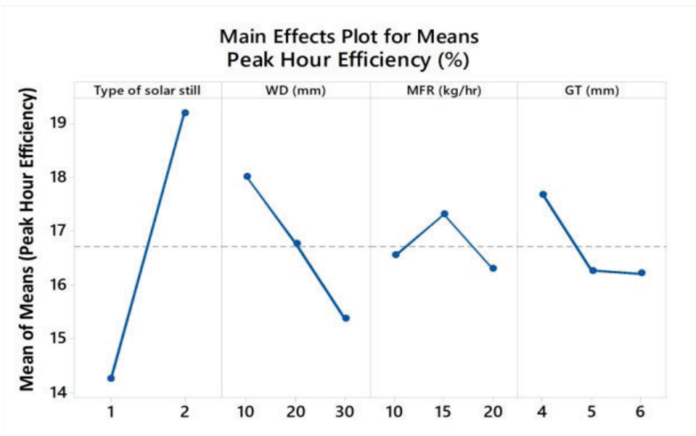

FIGURE 6. Mean of means for peak hour efficiency

In Figure 6, the main effects plot for means for peak hour efficiency is presented, illustrating the impact of various factors, including the type of solar still (SS), water depth, mass flow rate, and glass thickness, on peak hour efficiency. The response tables for the mean are presented in Table 6.

TABLE 6. Response table of means for peak hour efficiency

Level	TYPE OF SS	WD (mm)	MFR (kg/h)	GT (mm)
1	14.26	18.02	16.55	17.68
2	19.19	16.77	17.32	16.27
3		15.38	16.30	16.22
Delta	4.93	2.63	1.02	1.47
Rank	1	2	4	3

Based on the findings from Response Table 6, the solar still type had the maximum effect on peak hour efficiency, whereas the mass flow rate had the minimum effect on peak hour efficiency. The order of effectiveness of the parameters was as follows: type of solar still (SS) > water depth > glass thickness > mass flow rate.

Analysis of the SN ratio curve and means of means revealed that optimal (maximum) productivity and peak hour efficiency were attained when the type of solar still (SS) was set to 2, the water depth was 10 mm, the mass flow rate was 15 kg/h, and the glass thickness was 4 mm. This configuration is referred to as an optimal set of parameters. Table 7 presents the validation of responses for the optimal set of parameters. The predicted values of productivity and peak hour efficiency with the optimum set of parameters were 3881 ml and 22.03%, respectively. The experimentally obtained values for productivity and peak hour efficiency with the optimum set of parameters were 3913 ml and 22.14%, respectively. The prediction errors in productivity and peak hour efficiency were 0.81% and 0.49%, respectively, indicating that the Taguchi model had a better capacity to predict the results.

TABLE 7. Validation of predicted response for optimum set of parameters

Parameter	Optimum Set of Parameter				Experimented Value	Predicted Value	Error %
	Type of SS	WD (mm)	MFR (kg/h)	GT (mm)			
Productivity (ml)	2	10	15	4	3913	3881	0.81
Peak Hour Efficiency (%)	2	10	15	4	22.14	22.03	0.49

CONCLUSIONS

The Taguchi methods have effectively minimized the time and effort required for the evaluation and optimization of the design variables of solar stills.

1. The efficiency and productivity of stepped solar stills are higher than those of conventional stills.
2. The order of effectiveness of the parameters in terms of productivity and peak hour efficiency was as follows: type of solar still (SS) > water depth > glass thickness > mass flow rate.
3. Analysis of the SN ratio curve and means of means revealed that optimal maximum productivity and peak hour efficiency were attained when using a stepped solar still with a water depth of 10 mm, mass flow rate of 15 kg/h, and glass thickness of 4 mm.
4. The predicted values of productivity and peak hour efficiency with the optimum set of parameters were 3881 ml and 22.03%, respectively.

5. The experimentally obtained values for productivity and peak hour efficiency with the optimum set of parameters were 3913 ml and 22.14%, respectively.
6. The prediction errors in productivity and peak hour efficiency were 0.81% and 0.49%, respectively, suggesting that the Taguchi model demonstrated a better capacity to predict the results.

ACKNOWLEDGMENT

We extend our heartfelt gratitude to LDRP-ITR, Gandhinagar, for their generous provision of experimental facilities, which have been instrumental in advancing our research endeavors.

DECLARATION OF COMPETING INTEREST

None.

REFERENCES

Abebe, D.G. and Bogale, T.M. 2023. Optimization of TIG welding process parameters on 304 austenitic stainless steel sheet metal using fuzzy logic based Taguchi method. *Engineering Research Express* 5(4): 045045.

Ahmed, O.K., Daoud, R.W., Bawa, S.M., Ahmed, A.H. 2020. Optimization of PV/T Solar Water Collector based on Fuzzy Logic Control. *International Journal of Renewable Energy Development* 9(2): 303-310.

Berisha, Xh., Zeqiri, A. and Meha, D. 2018. Determining the optimum tilt angles to maximize the incident solar radiation - Case of Study Pristina. *Int. Journal of Renewable Energy Development* 7(2): 123-130.

Du, Y., He, G., Zhou, Z., Xu, L. and Huang, M. 2023. Multi-objective optimization of process parameters of laser cladding 15-5PH alloy powder based on gray-fuzzy taguchi approach. *Engineering Research Express* 5(2): 025015.

Dwivedi, V.K. and Tiwari, G.N. 2009. Comparison of internal heat transfer coefficients in passive solar stills by different thermal models: An experimental validation. *Desalination* 246(1-3): 304-318.

Elshamy, S.M. and El-Said, E.M. 2018. Comparative study based on thermal, exergetic and economic analyses of a tubular solar still with semi-circular corrugated absorber. *Journal of Cleaner Production* 195: 328-339.

Fatriasari, W., Hamzah, F.N., Pratomo, B.I., Fajriutami, T., Ermawar, R.A., Falah, F., Laksana, R.P.B., Ghozali, M., Iswanto, A.H., Hermiati, E., Winarni, I. 2020 Optimizing the synthesis of lignin derivatives from acacia mangium to improve the enzymatic hydrolysis of kraft pulp sorghum bagasse. *International Journal of Renewable Energy Development* 9(2): 227-235

Gnanaraj, S. J. P., & Ramachandran, S. 2017. Optimization on performance of single-slope solar still linked solar pond via Taguchi method. *Desalination and Water Treatment* 80: 27-40.

Ghasempour, R., Nazari, M.A., Ebrahimi, M., Ahmadi, M.H. and Hadiyanto, H. 2019. Multi-Criteria Decision Making (MCDM) approach for selecting solar plants site and technology: A review. *Int Journal of Renewable Energy Development* 8(1): 15-25.

Grewal, R. and Kumar, M. 2022a. Assessment of a solar powered sustainable energy recovery system for cleaner production of concentrated sugarcane juice. *Sustainable Energy Technologies and Assessments* 52: 102271.

Grewal, R. and Kumar, M. 2022b. Efficacy of mass of energy storage material on the performance of a solar driven stepped series system during sugarcane juice concentration. *Solar Energy* 243: 300-314.

Grewal, R. and Kumar, M. 2022c. Performance evaluation of a concatenated stepped solar still system loaded with different masses of energy storage material. *Energy* 259: 125005.

Hansen, R.S. and Murugavel, K.K. 2017. Enhancement of integrated solar still using different new absorber configurations: An experimental approach. *Desalination* 422: 59-67.

Ibrahim, S.N.H, and Hamza, E.A. 2017. Optimization of lipid extraction from municipal scum sludge for biodiesel production using statistical approach. *International Journal of Renewable Energy Development* 6(2): 171-179.

Jani, H.K. and Modi, K.V. 2017. Techniques of improving rate of heat transfer in Solar Still as a Solar-Thermal Desalination device–A Review. *Int. J. Adv. Res. Innov. Ideas Educ*. 3(2): 2395-4396.

Jani, H.K. and Modi, K.V. 2018. A review on numerous means of enhancing heat transfer rate in solar-thermal based desalination devices. *Renewable and Sustainable Energy Reviews* 93: 302-317.

Jani, H.K. and Modi, K.V. 2019 Experimental performance evaluation of single basin dual slope solar still with circular and square cross-sectional hollow fins. *Solar Energy* 179: 186-194.

Kabeel, A.E., Abdelgaied, M. and Sathyamurthy, R. 2019. A comprehensive investigation of the optimization cooling technique for improving the performance of PV module with reflectors under Egyptian conditions. *Solar Energy* 186: 257-263.

Karn, A.K., Agrawal, R., Kumar, A. and Mukhopadhyay, A. 2023. Deposition and process parameter optimization of electroless Ni-B coating from a stabilizer free bath to achieve enhanced microhardness, scratch-hardness and adhesion using taguchi's methodology. *Engineering Research Express* 5(3): 035036.

Kumar, P.V., Kumar, A., Prakash, O. and Kaviti, A.K. 2015. Solar stills system design: A review. *Renewable and Sustainable Energyreviews* 51: 153-181.

Kumar, A., & Kumar, R. 2024. Exergetic investigation and Taguchi-based optimization of a modified passive solar still augmented with nano-PCM & fins. *Journal of Energy Storage* 78: 109935.

Kumaravel, S., Nagaraj, M., & Barmavatu, P. 2024. Experimental and theoretical investigation to optimize the performance of solar still. *Desalination and Water Treatment*, 100343.

Le, T.H.,Pham, M.T., Hadiyanto, H., Pham, V.V., Hoang, A.T. 2021. Influence of various basin types on performance of passive solar still: A review. *International Journal of Renewable Energy Development* 10(2): 789-802.

Malik, M., Tiwari, G., Sodha, M. and Kumar, A. 1982. Solar energy conversion and photo energy systems. *Solar Distillation* 2: 1-10.

Manikandan, V., Shanmugasundaram, K., Shanmugan, S., Janarthanan, B. and Chandrasekaran, J. 2013. Wick type solar stills: A review. *Renewable and Sustainable Energy Reviews* 20: 322-335.

Modi, K.V. and Modi, J.G. 2019. Performance of single-slope double-basin solar stills with small pile of wick materials. *Applied Thermal Engineering* 149: 723-730.

Modi, K.V. and Nayi, K.H. 2020. Efficacy of forced condensation and forced evaporation with thermal energy storage material on square pyramid solar still. *Renewable Energy* 153: 1307-1319.

Modi, K.V., Nayi, K.H. and Sharma, S.S. 2020. Influence of water mass on the performance of spherical basin solar still integrated with parabolic reflector. *Groundwater for Sustainable Development* 10: 100299.

Mugaggaa, G. R., Omosab, I. B., & Thoruwa, T. 2023. Optimization and analysis of a low-pressure water scrubbing biogas upgrading system via the taguchi and response surface methodology approaches. *International Journal of Renewable Energy Development* 12(1): 99-110.

Nayi, K.H. and Modi, K.V. 2019. Thermal modeling of pyramid solar still. *Solar Desalination Technology*, 205-218.

Nayi, K.H. and Modi, K.V. 2021. Effect of cost-free energy storage material and saline water depth on the performance of square pyramid solar still: a mathematical and experimental study. *Journal of Thermal Analysis and Calorimetry* 144(4): 1351-1368.

Patel, K., Acharya, S. and Acharya, G.D. 2024a. Multi objective optimization of FDM parameters using taguchi grey relation analysis for PLA specimen. *Jurnal Kejuruteraan* 36(1): 113-122.

Patel, K., Acharya, S. and Acharya, G.D. 2024b. Taguchi grey relational analysis for multi-objective FDM parameter optimization of PLA components. *Jurnal Kejuruteraan* 36(3): 1155-1165.

Patel, R.V., Bharti, K., Singh, G., Kumar, R., Chhabra, S. and Singh, D.B. 2021. Solar still performance investigation by incorporating the shape of basin liner: A short review. *Materials Today: Proceeding* 43: 597-604.

Patel, T.M. and Bhatt, N.M. 2015. FEM based Taguchi method to reduce the automobile structural member weight. *GIT-Journal of Engineering and Technology* 8(1): 1-10.

Rahbar, N., Esfahani, J.A. and Asadi, A. 2016. An experimental investigation on productivity and performance of a new improved design portable asymmetrical solar still utilizing thermoelectric modules. *Energy Conversion and Management* 118: 55-62.

Rufuss, D.D.W., Iniyan, S., Suganthi, L. and Davies, P.A. 2016. Solar stills: A comprehensive review of designs, performance and material advances. *Renewable and Sustainable Energy Reviews* 63:464-496.

Sathyamurthy, R., Samuel, D.H., Nagarajan, P.K. and El-Agouz, S.A. 2015. A review of different solar still for augmenting fresh water yield. *Journal of Environmental Science and Technology* 8(6): pp.244-265.

Tabrizi, F.F., Dashtban, M., Moghaddam, H. and Razzaghi, K. 2010. Effect of water flow rate on internal heat and mass transfer and daily productivity of a weir-type cascade solar still. *Desalination* 260(1-3): 239-247.

Thakkar, H., Mevada, D. and Panchal, H. 2024. A Development in solar desalination system with flashing of solar heated water. *Jurnal Kejuruteraan* 36(2): 615-623.

Tiwari, G.N., Singh, H.N. and Tripathi, R. 2003. Present status of solar distillation. *Solar Energy* 75(5): 367-373.

Yadav, S. and Sudhakar, K. 2015. Different domestic designs of solar stills: A review. *Renewable and Sustainable Energy Reviews* 47: 718-731.

Yallese, M.A., Boucherit, S., Kouahla, I. and Belhadi, S. 2023. Multi-objective optimization of inconel 718 turning parameters using PCA-MARCOS and MARCOS-Taguchi. *Engineering Research Express* 5(3): 035043.